Published in final edited form as:
Free Radic Biol Med. 2013 December ; 65: . doi:10.1016/j.freeradbiomed.2013.07.005.

Characterization of NADPH oxidase 5 expression in human tumors and tumor cell lines with a novel mouse monoclonal antibody

Smitha Antony[1], **Yongzhong Wu**[1], **Stephen M. Hewitt**[3], **Miriam R. Anver**[4], **Donna Butcher**[4], **Guojian Jiang**[1], **Jennifer L. Meitzler**[1], **Han Liu**[2], **Agnes Juhasz**[1], **Jiamo Lu**[1], **Krishnendu K. Roy**[2], and **James H. Doroshow**[1,2]

[1]Laboratory of Molecular Pharmacology, Center for Cancer Research, National Cancer Institute, NIH, Bethesda, MD 20892

[2]Division of Cancer Treatment and Diagnosis, National Cancer Institute, NIH, Bethesda, MD 20892

[3]Laboratory of Pathology, National Cancer Institute, NIH, Bethesda, MD 20892

[4]Pathology/Histotechnology Laboratory, SAIC Frederick, Inc./Frederick National Laboratory for Cancer Research, NIH, Frederick, MD 21702

Abstract

Reactive oxygen species generated by NADPH oxidase 5 (Nox5) have been implicated in physiological and pathophysiological signaling pathways, including cancer development and progression. However, because immunological tools are lacking, knowledge of the role of Nox5 in tumor biology has been limited; the expression of Nox5 protein across tumors and normal tissues is essentially unknown. Here, we report the characterization and use of a mouse monoclonal antibody against a recombinant Nox5 protein (600–746) for expression profiling of Nox5 in human tumors by tissue microarray analysis. Using our novel antibody, we also report the detection of endogenous Nox5 protein in human UACC-257 melanoma cells. Immunofluorescence, confocal microscopy, and immunohistochemical techniques were employed to demonstrate Nox5 localization throughout UACC-257 cells, with perinuclear enhancement. Tissue microarray analysis revealed, for the first time, substantial Nox5 overexpression in several human cancers including those of prostate, breast, colon, lung, brain, and ovary as well as in malignant melanoma and non-Hodgkin lymphoma; expression in most non-malignant tissues was negative to weak. This validated mouse monoclonal antibody will promote further exploration of the functional significance of Nox5 in human pathophysiology, including tumor cell growth and proliferation.

To whom correspondence should be addressed: James H. Doroshow M.D., Division of Cancer Treatment and Diagnosis, Building 31, Room 3A44, National Cancer Institute, National Institutes of Health, 31 Center Drive, Bethesda, MD 20892 USA; Phone: (301) 496-4291; Fax: (301) 496-0826; doroshoj@mail.NIH.gov.

Conflict of interest

All authors have no personal, financial or commercial interest related to the development of the antibody.

Keywords

NADPH oxidase 5; tissue microarray; mouse monoclonal Nox5 antibody; melanoma; UACC-257 cells; reactive oxygen species; superoxide

Introduction

Compelling experimental evidence indicates that reactive oxygen species (ROS) function as intracellular second messengers activating opposing signaling cascades that can either be tumorigenic or lead to pathological tissue damage [1–10]. In a variety of rapidly growing human tumors high levels of ROS, particularly superoxide and hydrogen peroxide (H_2O_2) have been detected; in the appropriate context either or both may be essential for the initiation and the maintenance phases of tumor development [11–21]. One of the major sources of ROS is the NADPH oxidase (Nox) family of enzymes that is comprised of seven members, Nox 1–5 and dual oxidase (Duox) 1 and −2 that show distinct tissue distribution and mechanism of activation [22–41]. When human tumors have been compared to adjacent normal tissues, and in certain cultured cancer cell lines, increased mRNA expression of Nox1, 2, 4, and 5 or their regulatory components has been detected [2, 24, 42]. Of the Nox homologues, most studies have been carried out with Nox1 and Nox4 enzymes, the isoforms that, to date, have been most frequently implicated in cancer and pathologic inflammatory states [43–59].

Unlike Nox1, Nox2, and Nox4, the lack of Nox5 in the genome of rodents has contributed to a paucity of *in vivo* studies concerning the possible involvement of Nox5 in the development and progression of cancer. The function of Nox5 has, thus, largely been investigated in cell culture, and only to a limited degree in tissues [60, 61]. In human tumors, Nox5 expression has been demonstrated in hairy cell leukemia (mature B cells) but not in the normal circulating B-cell compartment [62]. Elevated Nox5 levels have also been found in some breast tumors relative to the adjacent non-tumor tissue as well as in several breast cancer cell lines [24]. In prostate cancer cell lines, regulation of growth and apoptosis by Nox5 has been reported [63, 64]. A role for Nox5 in cancer has been characterized best in Barrett's esophageal adenocarcinoma, where Nox5 is overexpresssed, and its expression has been found to be regulated by acid; in this context, enhanced Nox5-related ROS production could contribute to the role of chronic gastroesophageal reflux in the development of esophageal cancer [65, 66]. Additionally, Nox5 has also been implicated in the proliferation of endothelial cells and angiogenesis, and in PDGF-induced proliferation of vascular smooth muscle cells, processes that may enhance malignant progression [67–69].

Although there is a growing base of information regarding Nox5 regulation, signaling, and various biological functions, the role of Nox5-generated ROS in tumor biology is still largely unexplored. One of the factors limiting the progress of researchers in the Nox field is the lack of reliable antibodies. Since the first report of the cloning of Nox5 in 2001 and the subsequent generation of rabbit polyclonal antisera to Nox5 in 2003 [33, 35, 63], additional polyclonal antibodies for Nox5 detection have been reported [30, 70–76]. However, the absence of a reliable and well-characterized monoclonal antibody to Nox5 has impeded progress in this field. As reviewed by Bedard et al., studies on the expression of Nox5 in cancer cells are limited, and those across tumor tissues almost unknown [61]. Additionally, studies that report Nox5 expression in tumor tissues, namely for prostate adenocarcinoma and Barrett esophagus with dysplasia, were performed using real time RT-PCR.

To address the need for reliable immunological tools for Nox5 detection, we report here the characterization and use of the first mouse monoclonal antibody raised against a truncated

recombinant protein (residues 600–746) of Nox5. To obtain additional insights into the use of this antibody, we profiled Nox5 expression in human cancer using human tumor tissue microarrays. Screening of human tissue microarrays with this Nox5-specific antibody revealed substantial overexpression of Nox5 in a several human cancers, and to some extent, in cancers associated with inflammatory responses.

Materials

Anti-β-actin antibody (#A3853) and Triton® X-100 (T8787) were purchased from Sigma-Aldrich (St. Louis, MO); Anti-HA antibody (#11867423001) was purchased from Roche-Applied Science (Indianapolis, IN); and Hsp90 (#4877), PTP1B (#5311), PARP (#9532), and vimentin (#3390) antibodies were purchased from Cell Signaling (Danvers, MA). Normal mouse IgG (#sc-2025) was purchased from Santa Cruz Biotechnology (Santa Cruz, CA). Qproteome® cell compartment kit (#37502) was purchased from Qiagen (Valencia, CA). Alexa Fluor 488 goat-anti mouse IgG (#A11029), Stealth RNAi Negative Control Duplexes (#12935-100), Stealth Select RNAi™ siRNA for Nox5 (#HSS128401, HSS128402, HSS128403), Lipofectamine™ RNAiMAX (#13778-075) and Opti-MEM® Reduced serum medium (#11058-021) were from Invitrogen (Carlsbad, CA). The human primers for Nox1 (assay ID Hs00246589), Nox2 (assay ID Hs00166163), Nox4 (assay ID Hs00276431), Nox5 (assay ID Hs00225846), Duox1 (assay ID Hs00213694), Duox2 (assay ID Hs00204187_m1), human actin primer (assay ID Hs99999903_m1), and TaqMan Universal PCR mix (#4304437) were purchased from Applied Biosystems (Foster City, CA). Lab-Tek II 4-well glass chamber slides w/covers (#154917) were from Nalge Nunc International (Naperville, IL). Paraformaldehyde 20% solution (#15713-S) was purchased from Electron Microscopy Sciences, Inc., (Hatfield, PA). PI/RNase staining buffer (#550825) was purchased from BD Pharmingen™ (San Diego, CA). Vectashield mounting medium for fluorescence (#H-1000) was purchased from Vector Laboratories (Burlingame, CA). Myc-DDK-tagged-Nox2 plasmid (#RC207544) and Myc-DDK-tagged-Nox4 plasmid (#RC208007) were obtained from Origene (Rockville, MD). Nox5β (accession number AF325189) subcloned into a modified pcDNA3.1 containing an N-terminal HA epitope was a kind gift from Dr. David J. R. Fulton (Medical College of Georgia). A mouse monoclonal Nox1 antibody (Nox1-Hyb-Clone-22) was raised against a truncated recombinant protein representing the carboxyl-terminus 341 amino acids (224–564 amino acid sequence) of the human Nox1 protein [77]. Anti-D tag antibody (#G191) purchased from Applied Biological Materials Inc. (Richmond, BC, Canada) was used to detect DDK-tagged-Nox2/gp91-phox protein; and Myc-tag antibody (#2276) used to detect Myc-tagged-Nox4 protein was purchased from Cell Signaling Technology, Inc. (Danvers, MA). Duox protein was detected by immunoblot using a mouse monoclonal antibody S-40 that was raised against the human Duox2 131–540 amino acid fragment [78].

Instrumentation

To validate the specificity of the generated mouse monoclonal antibody against Nox5, several techniques were employed. Immunodetection by flow cytometry was measured on a FACScalibur (Becton Dickinson Biosciences, San Jose, CA) cytometer, acquired using the data file acquisition program CellQuest (Becton Dickinson Biosciences, San Jose, CA), and analyzed using the FlowJo software. Confocal microscopy for immunodetection of Nox5 antibody staining was visualized using an Olympus FluoView™ 300 confocal microscope scanning unit equipped with an argon-krypton laser at 488 nm mounted on an Olympus reflected fluorescence microscope (Olympus, Nagano, Japan). All images were obtained using the FluoView software (Olympus, Nagano, Japan). For immunofluorescence images, the stained slides were digitally imaged at 20X and 40X using the Aperio ScanScope®. To evaluate the expression of Nox5 across human tumor tissues, tissue microarray analysis was

performed on a TARP Multi-tumor TMA, generation 3, (MTA-3). Steps employed are detailed in the **Protocol** section below.

Protocol

Generation of mouse monoclonal Nox5 antibody

Immunization of mice and Nox5 monoclonal antibody production were carried out by Creative Biolabs, Port Jefferson Station, NY, using the following procedure. A recombinant protein containing a 147 amino acid immunogenic fragment corresponding to the 600–746 amino acid region of human Nox5 was expressed in *Escherichia coli*. The protein was purified and used as the antigen to produce a monoclonal antibody (data not shown). Four Balb/c mice were immunized with Nox5-Trx Protein. After five rounds of immunization with the immunogen, the serum titer reached significance as tested by an ELISA with Nox5-Trx and Nox5-GST. Subsequent to hybridoma fusion, the anti-sera were collected and individual clones were picked. Initial ELISA screening of the clones with Nox5-Trx isolated 18 positive clones. These clones were rescreened a second time using Nox5-Trx and Trx-tag, of which 8 positive clones were selected and evaluated further. Iso-typing of the 8 clones identified 7 of them as IgG clones. The specificity of these 8 clones for Nox5 detection was evaluated by Western analysis.

Sequencing of the variable region of the Nox5 antibody

Total RNA was extracted from the Nox5 hybridoma clone #14 using RNeasy Mini Kit (#74104) from Qiagen (Valencia, CA) according to the manufacturer's protocol. RT-PCR was performed using the Qiagen® OneStep RT-PCR kit (#210210) with primer sets specific for amplifying the human heavy (V_H) and light (V_L) chains (data not shown). For each RNA sample, 12 individual heavy chain and 11 light chain RT-PCR reactions were set up using degenerate forward primers covering the leader sequences of the variable region and reverse primers to the constant region of the heavy and light chains. No restriction sites were engineered into the primers. The RT-PCR products obtained after the first-round of reaction were further amplified by a second-round of PCR reaction using semi-nested primers specific for the antibody variable region (data not shown). The amplified V_H and V_L fragments were electrophoresed on 2% low-melting-point agarose gels and the bands around 400–500 base pair in size (expected for the variable region) were excised and cloned into the pT7Blue plasmid vector. For both V_H and V_L, three independent clones were sequenced and the DNA sequence and the corresponding amino acid sequence of the complementarity determining regions (CDR) were analyzed.

Cell culture and transfection

The human melanoma cell lines LOX-IMVI and UACC-257 were obtained from the Developmental Therapeutics Program, Division of Cancer Treatment and Diagnosis of the National Cancer Institute, Bethesda, MD and were cultured in RPMI-1640 medium supplemented with 10% FBS. HEK-293 (#CRL-1573™), HT-29 (#HTB-38™), and BxPC-3 cells (#CRL-1687™) were obtained from ATCC (Manassas, VA) and cultured using ATCC recommended medium supplemented with 10% FBS and maintained at 37 °C in a humidified atmosphere of 5% CO_2 and 95% air. Transfection in cells was carried out using Lipofectamine® 2000 (#11668019) from Invitrogen (Carlsbad, CA) according to the manufacturer's protocol. To generate cells that stably overexpress Nox5, parental UACC-257 cells were transfected with a pcDNA3-HA-Nox5β plasmid or empty vector using Lipofectamine® 2000. Resistant clones were selected with 700 μg/ml G418, and then single clones were selected and maintained under G418 selection. For gene silencing experiments, log-phase UACC-257 cells were trypsinized and reverse transfected with 5 nM of either control or two different Nox5 Stealth Select RNAi's (#HSS 128401 and #HSS

128402) using the Lipofectamine™ RNAiMAX transfection reagent from Invitrogen (Carlsbad, CA). After 72 h of transfection, silencing efficiency was analyzed by measuring the level of Nox5 at the RNA level by TaqMan real-time PCR and/or protein level by immunoblotting. Stealth RNAi™ Negative Control Duplex was used as the negative control.

RNA Analysis: extraction, cDNA synthesis, and quantitative real time PCR assay

Total RNA was isolated from cells with the RNeasy Mini Kit (#74104) from Qiagen (Valencia, CA), according to the manufacturer's protocol. RNA was treated with a DNase kit (#79254) according to the manufacturer's specifications (Qiagen, Valencia, CA) so that all remaining DNA could be removed. RNA concentrations and purity were measured on the Nanodrop ND-1000 apparatus (Nanodrop Technologies, Wilmington, DE). Two μg of total RNA was used for cDNA synthesis using SuperScript II reverse transcriptase (#18080-044) and random primers (# 48190-011) from Invitrogen (Carlsbad, CA) in a 20 μl reaction system. The cycling conditions were as follows: 25 °C for 5 min, 42 °C for 50 min, 75 °C for 5 min. After reaction, the RT-PCR products were diluted with diethyl pyrocarbonate/ H_2O to 100 μl for the real time PCR. Real time RT-PCR was performed on 384-well plates in a 20-μl reaction system containing 2 μl of diluted cDNA, 1 μl of appropriate primer, 7 μl of H_2O, and 10 μl of TaqMan 2X gene expression master mix reagent (#4304437, Applied Biosystems, Foster City, CA). The PCR was carried out using the default cycling conditions, and fluorescence was detected with the ABI 7900HT sequence detection system (Applied Biosystems, Foster City, CA). Triplicate determinations were performed for each sample that was used for the real time PCR; the mean value was calculated, and the data in the final figures represents three independent experiments. Relative gene expression was calculated as the ratio of Nox5 gene expression to the internal reference gene (β-actin) multiplied by 10^6 based on the C_t values.

Preparation of subcellular fractions and whole cell lysate

Subcellular fractions of parental UACC-257 and Nox5 overexpressing UACC257 Clone 2 cells were prepared using the Qproteome cell compartment kit (#37502) from Qiagen (Valencia, CA). Briefly, 1.5×10^6 cells were transfected with either scrambled control siRNA or Nox5-specific siRNA-primer 1. After 72 h in culture, the cells were washed with ice-cold PBS buffer and then sequentially extracted using a combination of four extraction buffers and separated into cytosolic, membrane, nuclear, and cytoskeletal fractions according to the manufacturer's instructions. Immunoblotting with Hsp90, PTP1B, PARP, and vimentin antibodies specific for cytosolic, membrane, nuclear, and cytoskeleton proteins, respectively, verified the isolation of each fraction.

For whole cell lysate, cells were washed with ice-cold PBS, harvested and lysed with 1× RIPA lysis buffer (#20–188, Millipore, Temecula, CA) with the addition of a phosphatase inhibitor tablet (#04906845001, Roche Applied Science, Indianapolis, IN) and a protease inhibitor tablet (#11836153001, Roche Applied Science, Indianapolis, IN). Samples were sonicated 3 times for 5 s each (20 watts), and the lysates were cleared by centrifugation (6,000 × *g*, 10 min). Protein concentration was estimated using the BCA protein assay kit (#23227, Thermo Scientific, Rockford, IL), and bovine serum albumin (BSA) was used as the standard.

Western analysis

The subcellular fractions and whole cell lysates were mixed with an equal volume of 2× SDS protein gel loading buffer (#351-082–661, Quality Biological Inc, Gaithersburg, MD), and fractions (20 μg) or lysates (40 μg) of each were loaded onto a 4–20% Tris glycine gel (#EC6028, Invitrogen, Carlsbad, CA). For detection of Nox5 expression, the fractions and lysates that were mixed with an equal volume of 2× SDS loading buffer were not heated

prior to loading onto gels. Subsequent to gel separation, the proteins were electrophoretically transferred onto nitrocellulose membranes using I Blot gel transfer stacks (#IB 3010-01, Invitrogen, Carlsbad, CA). The membranes were blocked in 1× TBST buffer with 5% nonfat milk for 1 h at room temperature followed by incubation with the primary antibody overnight in TBST buffer. Membranes were washed three times in 1× TBST buffer and incubated with horseradish peroxidase-conjugated secondary antibody for 1 h at room temperature with shaking. The antigen-antibody complexes were visualized using the SuperSignal West Pico Luminol/Enhancer Solution (#1856136, Thermo Scientific, Rockford, IL).

Immunodetection by flow cytometry

Log phase UACC-257 cells that stably overexpress Nox5 (Clone 2) or the vector control (Clone 1) were trypsinized, washed in cold PBS, pelleted and then resuspended in cold PBS/FBS solution (PBS containing 5% fetal bovine serum and 1% sodium azide). Cells were centrifuged for 5 min at 250 × *g* and then fixed with cold 2% (w/v) paraformaldehyde for 30 min on ice. Following centrifugation, the cells were permeabilized by resuspending the pellet in room temperature Tween 20 solution (0.2% in PBS) for 15 min in a 37 °C water bath. After centrifugation, cells (10^6) were either unlabeled and resuspended in PBS or labeled with irrelevant mouse IgG antibody (5 μg) or Nox5 specific mouse monoclonal antibody (5 μg) in human AB serum (heat-inactivated) for 30 min at 4 °C in the dark. The labeled cells were then washed twice with Tween solution (0.2% in PBS) followed by incubation with secondary Alexa Fluor 488 goat anti-mouse antibody [diluted 1:1000 in human AB serum (heat-inactivated)] for 20 min on ice in the dark. Cells were then centrifuged, washed twice with Tween solution (0.2% in PBS), and resuspended in PBS. Fluorescence intensity of the cells was measured on a FACScalibur (Becton Dickinson Biosciences, San Jose, CA) cytometer and acquired using the data file acquisition program CellQuest (Becton Dickinson Biosciences, San Jose, CA) and analyzed using the FlowJo software.

Immunodetection by confocal microscopy

5×10^3 UACC-257 cells or UACC-257-clone 2 cells that stably overexpress Nox5 were transfected with either scrambled control siRNA or Nox5-specific siRNAs and seeded onto chamber slides. 72 h after transfection, they were fixed with 4% (w/v) paraformaldehyde for 10 min at room temperature. After two washes with PBS, cells were permeabilized with 0.1% Triton X-100 (v/v) for 5 min at room temperature. Following two washes with PBS containing 1% (w/v) BSA, the cells were blocked with PBS containing 8% (w/v) BSA for 1 h. After two further washes, the cells were incubated overnight at 4 °C with the mouse monoclonal Nox5 antibody (1:1000 for Fig. 7A and 1:10,000 for Fig. 7B) diluted in 400 μl of PBS containing 1% (w/v) BSA. For negative controls, cells were incubated with isotype-matched mouse IgG. Following washes, a secondary Alexa Fluor 488 goat anti-mouse antibody [1:1000 in PBS containing 1% (w/v) BSA] was added. After a 1 h-incubation, cells were washed, and the cell nuclei were stained with propidium iodide (PI, 0.5 μg/ml). Samples were then mounted in Vectashield solution, sealed, and stored at 4 °C in the dark. Confocal microscopy was carried out using an Olympus FluoView™ 300 confocal microscope scanning unit equipped with an argon-krypton laser at 488 nm mounted on an Olympus reflected fluorescence microscope (Olympus, Nagano, Japan). All images were obtained using the FluoView software (Olympus, Nagano, Japan).

Immunohistochemistry

Pellets of UACC-257 cells that stably overexpress HA-tagged Nox5 protein (Clone 2) or the vector control (Clone 1), and the LOX-IMVI cells that express none/minimal Nox5 were

fixed in 10% buffered neutral formalin and used as immunohistochemistry controls to optimize conditions for Nox5 immunohistochemistry. Optimal conditions were at a Nox5 dilution of 1:1000 with heat-induced epitope retrieval in citrate buffer for 20 min; the incubation time was 30 minutes for the primary antibody. We also used a biotinylated secondary horse anti-mouse IgG (Vector Laboratories) and the Intense RD Detection kit from Leica Biosystems. Slides were run on a Leica Bond Autostainer. Isotype control was normal mouse IgG2a (BD Bioscience) at a comparable concentration.

Following immunostaining, slides were bleached with hydrogen peroxide/potassium hydroxide for 60 min at 37 °C followed by a 20 second acetic acid rinse to eliminate melanin pigment. After bleaching, slides were counter-stained with hematoxylin. Slides were digitally imaged at 20X and 40X using the Aperio ScanScope®.

Normal Human Tissue

Unstained slides of formalin-fixed paraffin embedded normal human uterus were purchased from Pantomics. Nox5 staining conditions and controls (mouse IgG2a) are similar to those detailed above for immunohistochemistry except that bleaching was not done. Other normal human tissues tested were colon, liver, spleen and testis.

Tissue microarray

Immunohistochemistry was performed on a TARP Multi-tumor TMA, generation 3, (MTA-3). The TMA was deparaffinized in alcohol and rehydrated with graded alcohol. The slide was subject to antigen retrieval with pH 9 antigen retrieval buffer (Dako) for 20 min in a pressure cooker. The anti-Nox5 antibody was applied at a dilution of 1:2000 for 4 h at room temperature, and the antigen-antibody reaction was detected with the Envision+ detection system (Dako), with DAB chromagen. The slide was counterstained with hematoxylin, dehydrated and cover slipped. The assay was interpreted with a scoring system of 0, 1, 2, and 3, for cytoplasmic staining corresponding to negative, weak, intermediate, and strong staining.

Statistical analysis

Results are expressed as the mean ± S.D. from at least triplicate experiments. Statistical differences between mean values of control and treated samples were assessed using Student's *t* test; $p < 0.05$ was considered statistically significant. Significance levels were designated as *, $p < 0.05$; **, $p < 0.01$ throughout.

Expected Results

Monoclonal anti-Nox5 peptide production and detection of endogenous Nox5 in human UACC-257 melanoma cells

The mouse monoclonal antibody was raised against a truncated recombinant protein (residues 600–746) of the Nox5 protein (Fig. 1, highlighted in pink). After five rounds of immunization in mice and two preliminary rounds of screening, clones that were positive for Nox5 antibody production by ELISA (Supplementary Table 1) were further evaluated by Western analysis. Five of eight clones were positive for Nox5 protein detection by Western (Supplementary Fig. 1), of which clone #14 was used for this study subsequent to purification on peptide-affinity columns. As shown in Fig. 2A, the human melanoma UACC-257 cell line expresses reasonable levels of endogenous Nox5 mRNA levels as detected by RT-PCR. Screening of the affinity purified Nox5 mouse monoclonal antibody (1:1000 dilution in 2.5% milk-TBST) by Western blotting of UACC-257 cell lysates demonstrated a reactive band with molecular weight of ~ 75 kDa (Fig. 2B). The displayed

reactivity on immunoblots decreased in intensity when the UACC-257 cells were transiently transfected with two different Nox5-specific siRNAs 1 and 2 (see Fig. 2B) in comparison to those transfected with non-specific scrambled siRNA. The observed decrease in protein expression (Fig. 2B) also corresponded to levels of Nox5 mRNA expression (Fig. 2A), confirming the detected band as denatured Nox5 protein.

Specificity of the affinity-purified mouse monoclonal antibody for human Nox5 protein

To validate the specificity of the monoclonal antibody for Nox5, UACC-257 cells that stably overexpress HA-tagged Nox5 protein or the vector control were generated. Of the several G418 positive clones selected, two vector clones (1 and 2) and two Nox5 overexpressing clones (1 and 2) were used for this study. The Nox5 overexpressing clones (1 and 2) express ~ 35–50 times more Nox5 mRNA than either the parental UACC-257 cells or the vector transfected clones (Fig. 3A). As observed in Fig. 3B (top panel), the Nox5 monoclonal antibody (1:10,000) detects an intense band corresponding to ~ 75 kDa in the Nox5 overexpressing clones. A similar sized band can be detected in the parental and vector control cells upon longer exposure of the immunoblot (Fig 3B, Nox5 dark). Probing the stripped blots with HA confirmed the detected band to be HA-tagged-Nox5 protein. Additionally, stable, Nox5 overexpressing clone 2 cells were transiently knocked down for Nox5 expression with two different Nox5-specific siRNAs, as confirmed by RT-PCR (Fig. 3D). The decrease of Nox5 transcription observed in Nox5-siRNA samples compared to the untransfected and scrambled siRNA transfected controls also translated to a corresponding decrease in the Nox5 protein expression (Fig. 3C, top panel). HA-tag staining of the stripped blots confirmed the decrease in expression levels of Nox5 (Fig.3C, middle panel), validating the specificity of the antibody for human Nox5.

To determine the cross-reactivity of our mouse monoclonal Nox5 antibody for other homologues of the NADPH (Nox) family, Western analysis was carried out using samples positive for Nox1 (HT-29 colon cancer cell line), Nox2 (HEK-293 transiently transfected with DDK-tagged Nox2 plasmid), Nox4 (HEK293 cells transiently transfected with Myc-tagged Nox4 plasmid), Nox5 (UACC-257 cells and HA-tagged Nox5 overexpressing cells), and Duox (BxPC-3 pancreatic cells untreated or treated with 25 ng/ml IFN-γ for 24 h) expression. A Nox3 positive sample was not tested because its expression is minimal in human tumors. As observed in Fig. 4, the Nox5 mouse monoclonal antibody specifically recognizes only the Nox5 protein.

Immunodetection of endogenous and recombinant Nox5 protein in membrane fractions of UACC-257 cells

Parental UACC-257 cells and stable, Nox5-overexpressing clone 2 cells were transiently transfected with either a scrambled siRNA or a Nox5-specific siRNA. The cell lysates were separated into cytosolic, membrane, nuclear, and cytoskeletal fractions as described in the Protocol section. As shown in Figs. 5A and B, Nox5 is primarily present in the membrane fraction. The fractionation methodology was validated by confirming the presence of Hsp90 in the cytosol, PTP1B in the membrane fraction, poly(ADP-ribose) polymerase (PARP) in the nucleus, and vimentin in the cytoskeletal fraction (Figs. 5A and B). Absence/decrease of Nox5 expression in the presence of Nox5 siRNA (lane 6 of Figs. 5A and B) in both parental UACC-257 cells and Nox5-overexpressing clone 2, confirms that Nox5 is predominately present in the membrane fraction.

Monoclonal antibody recognizes the intracellular domain of Nox5

The binding of the monoclonal antibody to native antigen was further investigated by flow cytometry on intact and permeabilized UACC-257-Nox5 overexpressing cells. Fig. 6 shows that Tween-20 permeabilized Nox5-overexpressing cells demonstrate considerable antibody

bound to Nox5 when compared to vector control cells. However, no such differential expression of Nox5 was detected in vector control cells or in intact Nox5-overexpressing cells. This data confirms that our Nox5 mouse monoclonal antibody recognizes an intracellular epitope on Nox5 in support of its original design against the conserved carboxy-terminal of Nox5 from amino acid sequence 600–746 (Fig. 1).

The immunoreactivity of the mouse monoclonal antibody on an intracellular epitope of Nox5 can also be visualized by confocal microscopy (Figs. 7A and B). Permeabilized UACC-257 cells when stained with the mouse Nox5 monoclonal antibody (1:1000 dilution) demonstrate green fluorescent labeling for Nox5 localized throughout UACC-257 cells, with perinuclear enhancement suggestive of the endoplasmic reticulum. Control cultures treated identically except for the addition of primary antibodies or isotype specific (mouse IgG) control antibody showed no green fluorescence. Specificity for Nox5 was evident as Nox5 staining intensity was significantly decreased (>60%) in parental UACC-257 cells that were transiently transfected with two different Nox5-specific siRNAs as compared to those transfected with the scrambled siRNA (Fig. 7A). Likewise, as observed in Fig. 7B, UACC-257 cells that stably overexpress Nox5 (Clones 1 and 2) demonstrate cytoplasmic Nox5 staining with perinuclear enhancement with the mouse Nox5 monoclonal antibody (1:10,000 dilution) when compared to the parental UACC-257 and vector control (Clone 1 and 2) cells. The Nox5 staining observed in the Nox5 overexpressing cells was significantly decreased (>65%) upon transient knockdown of Nox5 expression (Fig. 7B). The intracellular staining pattern of Nox5 using our mouse monoclonal antibody was reflective of the expression levels of Nox5 within the cells. This, coupled with the fact that no significant Nox5 staining was observed in intact cells (data not shown), confirms the specificity of the antibody to an intracellular domain of Nox5.

Immunohistochemical validation of Nox5 mAb

Immunohistochemical reactivity of Nox5 monoclonal antibody on UACC-257-derived cell pellets was cytoplasmic with darker staining toward the cell membrane. Reactivity was strong and diffuse in the Nox5 over-expressers, weaker and patchier in the vector control UACC-257 pellets, while absent/weak in the Nox5 negative LOX-IMVI melanoma cell line (Fig. 8A). There was no immunoreactivity with the isotype control.

Additionally, to evaluate expression of Nox5 in normal human tissue, formalin-fixed paraffin embedded normal human uterus, colon, liver, spleen and testis were stained with the Nox5 monoclonal antibody. As shown in Fig. 8B, the human uterine smooth muscle had diffusely positive cytoplasmic staining with Nox5 while there was no reactivity with the mouse isotype control. Staining for Nox5 in normal human tumors was weak in colon, liver, testis and spleen (data not shown).

Tissue microarray

Expression of Nox5 in tumor tissues was evaluated by immunohistochemical staining of a TARP MTA-3 multitumor TMA (Fig. 9). The assay was interpreted with a scoring system of 0, 1, 2, and 3, for cytoplasmic staining of Nox5 corresponding to negative, weak, intermediate, and strong staining, respectively. The graphical distribution of each tumor scored by the intensity of Nox5 staining and tumor type is represented in Fig. 9B and the percentage distribution of positive staining (2 and 3) by tumor type for the multi-tumor TMA is shown in Table 1. Of the 382 evaluable tumor samples, 143 (38%) were negative (0) or weak (1) for Nox5 expression, while 239 (63%) were intermediate or strong (2 or 3) for Nox5. Expression within the normal tissues on the TMA revealed intermediate expression (2) limited to bone marrow, liver, pancreas and endometrium, with negative or weak expression (0–1) in the other tissues screened. Lymphomas had the lowest percentage

of Nox5 positive tumors (44%), while prostate cancer demonstrated the highest frequency of positive expression (81%). The remainder of tumors screened (brain tumors, melanoma, breast, colon, ovarian and lung cancer) had frequencies of intermediate or strong expression between 56–70%.

Caveats

Since the first report of the discovery of Nox5 in 2001, the expression of Nox5 has been documented at the mRNA level in a number of cancers or cancer cell lines including prostate, pancreatic, breast, melanoma, and esophageal cancer, as well as hairy cell leukemia [65, 66]. Although implicated in several malignancies, the role of Nox5 in tumor cell biology is still unclear. This is due, in part, to a lack of reliable immunological probes for Nox5 detection as well as the absence/limited studies of Nox5 in human tumor tissues. A lack of specificity and characterization of detection tools is a major caveat not limited to Nox5, but to the entire ROS-Nox field [4, 79]. In particular, concerns about the specificity (or lack thereof) of currently available commercial antibodies against Nox homologs have made interpretation of studies that solely rely on these antibodies difficult [4, 79]. To address this need, here we report the characterization and qualification of the first mouse monoclonal antibody against Nox5.

Our monoclonal antibody against Nox5 was raised in mice against a truncated recombinant protein (residues 600–746) of Nox5. As observed in Fig. 1 (highlighted in pink), the antibody is directed to an intracellular domain of Nox5, which is conserved across all of the known Nox5 variants. Subsequent to screening by ELISA and Western blotting (Supplementary Table 1 and Supplementary Fig. 1), the serum of immunized mice (clone #14) was used as a source for antibody purification on peptide-affinity columns. Sequencing of the purified antibody (as detailed in the Protocol section) confirmed the antibody from hybridoma clone #14 to contain one mouse heavy chain and one mouse light chain (Supplementary Fig. 2). The specificity of the purified antibody for Nox5 was determined by its reactivity under 3 different experimental conditions: 1) endogenous Nox5 expression in the UACC-257 melanoma cell line, 2) overexpressed HA-tagged Nox5, and 3) transient silencing of endogenous Nox5 and stably overexpressed Nox5. The purified antibody displayed reactivity to an ~ 75 kDa band on immunoblots (Figs. 2B, 3B and C), which was confirmed as denatured Nox5 protein by expression patterns that corresponded to transient Nox5 knockdown experiments (Figs. 2B, 3C) as well the HA-tag (Figs. 3 B and C). Additionally, the absence of cross-reactivity to other homologs of the NADPH oxidase family (see Fig. 4) confirmed the mouse monoclonal antibody to be Nox5-specific.

In conformity with the design of the antibody against the conserved carboxy-terminal of Nox5 (Fig. 1), a significant right shift in fluorescence intensity was observed by flow cytometry in permeabilized cells that overexpress Nox5 compared to a control vector; no shift in fluorescence was observed between vector control and Nox5 overexpressers in intact cells (Fig. 6), confirming antibody reactivity toward an intracellular epitope of Nox5. Subcellular fractionation of both UACC-257 melanoma cells and a Nox5-overexpressing UACC-257 clone demonstrate that Nox5 appears to be predominantly localized in the membrane fraction (Fig. 5). Confocal microscopy of labeled cells revealed green fluorescent labeling for Nox5 localized throughout UACC-257 cells, with perinuclear enhancement (Fig. 7).

A major concern in understanding the role of Nox5 in tumor biology is the lack of current studies on human tumor tissues. To evaluate the clinical significance of Nox5 in human cancer, we determined the expression of Nox5 protein in a representative set of human tumors, including those of brain, ovary, breast, colon, lung, and prostate, as well as in

malignant melanoma, and a panel of non-Hodgkin Lymphomas by tissue microarray analysis. Expression of Nox5 was detected in 63% of tumors evaluated, most frequently in prostate cancer (81%), but between 56–70% in 7 additional tumor types. The only tumor type evaluated in which Nox5 expression was less than 50% was lymphoma. Although the majority of tumor types screened are carcinomas, with a predominance of adenocarcinomas, the rates of expression in the brain tumor samples (glioblastoma multiforme) and melanoma do not suggest Nox5 expression is restricted to cancers of only certain tissue origins. Low expression of Nox5 in normal tissues, including the tissue of origin for many of the cancers screened, supports the hypothesis that Nox5 expression is upregulated in many human cancers (Fig. 9).

In summary, progress in the study of Nox proteins has been impeded by the paucity of well-validated immunological probes. Herein, we report the characterization and use of a mouse monoclonal antibody against Nox5 that can be employed for Western analysis, immunofluorescence, flow cytometry, and immunohistochemistry on fixed tissues. Using this antibody, we clarified the cellular location of Nox5 expression in a human melanoma cell line (membrane predominant) and examined Nox5 expression in human tumor microarrays. We found substantial overexpression of Nox5 in a variety of epithelial malignancies compared to normal tissues of the same organ. The elevated expression of Nox5 in tumor specimens provides impetus for further exploration of the functional significance of Nox5 in the context of tumor development and maintenance. By making this antibody widely available to the research community, we hope to increase understanding of the pathways that regulate Nox5 in cancer, leading to greater knowledge of the role of Nox-dependent ROS production and signal transduction in the progression of human malignancies. Ultimately, we hope that this reagent will assist in providing focus for the further development of Nox5 as a target of therapeutic significance.

Supplementary Material

Refer to Web version on PubMed Central for supplementary material.

Acknowledgments

This work was supported with federal funds from the Center for Cancer Research, the Division of Cancer Treatment and Diagnosis, and the NCI Contract No. HHSN261200800001E, National Cancer Institute, National Institutes of Health. The content of this publication does not necessarily reflect the views or policies of Health and Human Services, nor does mention of trade names, commercial products or organizations imply endorsement by the US Government.

Abbreviations used in the text

Nox	NADPH oxidase
ROS	reactive oxygen species

References

1. Burdon RH. Superoxide and hydrogen peroxide in relation to mammalian cell proliferation. Free Radical Biology and Medicine. 1995; 18:775–794. [PubMed: 7750801]
2. Block K, Gorin Y. Aiding and abetting roles of NOX oxidases in cellular transformation. Nat Rev Cancer. 2012; 12:627–637. [PubMed: 22918415]
3. Thannickal VJ, Fanburg BL. Reactive oxygen species in cell signaling. Am J Physiol Lung Cell Mol Physiol. 2000; 279:L1005–L1028. [PubMed: 11076791]

4. Altenhofer S, Kleikers PW, Radermacher KA, Scheurer P, Rob Hermans JJ, Schiffers P, et al. The NOX toolbox: validating the role of NADPH oxidases in physiology and disease. Cell Mol Life Sci. 2012; 69:2327–2343. [PubMed: 22648375]
5. Cui X. Reactive oxygen species: the achilles' heel of cancer cells? Antioxid Redox Signal. 2012; 16:1212–1214. [PubMed: 22304673]
6. Cui XL, Chang B, Myatt L. Expression and distribution of NADPH oxidase isoforms in human myometrium--role in angiotensin II-induced hypertrophy. Biol Reprod. 2010; 82:305–312. [PubMed: 19812300]
7. Montezano AC, Touyz RM. Oxidative stress, Noxs, and hypertension: experimental evidence and clinical controversies. Ann Med. 2012; 44(Suppl 1):2–16.
8. Oberley LW, Oberley TD, Buettner GR. Cell division in normal and transformed cells: the possible role of superoxide and hydrogen peroxide. Med Hypotheses. 1981; 7:21–42. [PubMed: 6259499]
9. Storz P. Reactive oxygen species in tumor progression. Front Biosci. 2005; 10:1881–1896. [PubMed: 15769673]
10. Rhee SG. Cell signaling. H2O2, a necessary evil for cell signaling. Science New York, NY. 2006; 312:1882–1883.
11. Luczak K, Balcerczyk A, Soszynski M, Bartosz G. Low concentration of oxidant and nitric oxide donors stimulate proliferation of human endothelial cells in vitro. Cell Biol Int. 2004; 28:483–486. [PubMed: 15223026]
12. Murrell GA, Francis MJ, Bromley L. Modulation of fibroblast proliferation by oxygen free radicals. Biochem J. 1990; 265:659–665. [PubMed: 2154966]
13. Tochhawng L, Shuo D, Pervaiz S, Yap CT. Redox regulation of cancer cell migration and invasion. Mitochondrion. 2012
14. Mu P, Liu Q, Zheng R. Biphasic regulation of H2O2 on angiogenesis implicated NADPH oxidase. Cell Biol Int. 2010; 34:1013–1020. [PubMed: 20575760]
15. Szatrowski TP, Nathan CF. Production of large amounts of hydrogen peroxide by human tumor cells. Cancer Res. 1991; 51:794–798. [PubMed: 1846317]
16. Bittinger F, Gonzalez-Garcia JL, Klein CL, Brochhausen C, Offner F, Kirkpatrick CJ. Production of superoxide by human malignant melanoma cells. Melanoma Res. 1998; 8:381–387. [PubMed: 9835450]
17. Lambeth JD. Nox enzymes, ROS, and chronic disease: an example of antagonistic pleiotropy. Free Radic Biol Med. 2007; 43:332–347. [PubMed: 17602948]
18. Sugamura K, Keaney JF Jr. Reactive oxygen species in cardiovascular disease. Free Radic Biol Med. 2011; 51:978–992. [PubMed: 21627987]
19. Novo E, Marra F, Zamara E, Valfre di BL, Caligiuri A, Cannito S, et al. Dose dependent and divergent effects of superoxide anion on cell death, proliferation, and migration of activated human hepatic stellate cells. Gut. 2006; 55:90–97. [PubMed: 16041064]
20. Kumar B, Koul S, Khandrika L, Meacham RB, Koul HK. Oxidative stress is inherent in prostate cancer cells and is required for aggressive phenotype. Cancer Res. 2008; 68:1777–1785. [PubMed: 18339858]
21. Fried L, Arbiser JL. The reactive oxygen-driven tumor: relevance to melanoma. Pigment Cell Melanoma Res. 2008; 21:117–122. [PubMed: 18384505]
22. Coso S, Harrison I, Harrison CB, Vinh A, Sobey CG, Drummond GR, et al. NADPH oxidases as regulators of tumor angiogenesis: current and emerging concepts. Antioxid Redox Signal. 2012; 16:1229–1247. [PubMed: 22229841]
23. Ushio-Fukai M. Redox signaling in angiogenesis: role of NADPH oxidase. Cardiovasc Res. 2006; 71:226–235. [PubMed: 16781692]
24. Juhasz A, Ge Y, Markel S, Chiu A, Matsumoto L, van Balgooy J, et al. Expression of NADPH oxidase homologues and accessory genes in human cancer cell lines, tumours and adjacent normal tissues. Free radical research. 2009; 43:523–532. [PubMed: 19431059]
25. Geiszt M. NADPH oxidases: new kids on the block. Cardiovasc Res. 2006; 71:289–299. [PubMed: 16765921]

26. Bedard K, Krause KH. The NOX family of ROS-generating NADPH oxidases: physiology and pathophysiology. Physiol Rev. 2007; 87:245–313. [PubMed: 17237347]
27. Lambeth JD, Kawahara T, Diebold B. Regulation of Nox and Duox enzymatic activity and expression. Free Radic Biol Med. 2007; 43:319–331. [PubMed: 17602947]
28. Hilenski LL, Clempus RE, Quinn MT, Lambeth JD, Griendling KK. Distinct subcellular localizations of Nox and Nox4 in vascular smooth muscle cells. Arterioscler Thromb Vasc Biol. 2004; 24:677–683. [PubMed: 14670934]
29. Krause KH. Tissue distribution and putative physiological function of NOX family NADPH oxidases. Jpn J Infect Dis. 2004; 57:S28–S29. [PubMed: 15507765]
30. Banfi B, Tirone F, Durussel I, Knisz J, Moskwa P, Molnar GZ, et al. Mechanism of Ca2+ activation of the NADPH oxidase 5 (NOX5). J Biol Chem. 2004; 279:18583–18591. [PubMed: 14982937]
31. Lambeth JD. NOX enzymes and the biology of reactive oxygen. Nat Rev Immunol. 2004; 4:181–189. [PubMed: 15039755]
32. Dewald B, Baggiolini M, Curnutte JT, Babior BM. Subcellular localization of the superoxide-forming enzyme in human neutrophils. J Clin Invest. 1979; 63:21–29. [PubMed: 216707]
33. Banfi B, Molnar G, Maturana A, Steger K, Hegedus B, Demaurex N, et al. A Ca(2+)-activated NADPH oxidase in testis, spleen, and lymph nodes. J Biol Chem. 2001; 276:37594–37601. [PubMed: 11483596]
34. Banfi B, Malgrange B, Knisz J, Steger K, Dubois-Dauphin M, Krause KH. NOX3, a superoxide-generating NADPH oxidase of the inner ear. J Biol Chem. 2004; 279:46065–74602. [PubMed: 15326186]
35. Cheng G, Cao Z, Xu X, van Meir EG, Lambeth JD. Homologs of gp91phox: cloning and tissue expression of Nox3, Nox4, and Nox5. Gene. 2001; 269:131–140. [PubMed: 11376945]
36. Cheng G, Ritsick D, Lambeth JD. Nox3 regulation by NOXO1, p47phox, and p67phox. J Biol Chem. 2004; 279:34250–34255. [PubMed: 15181005]
37. Dupuy C, Ohayon R, Valent A, Noel-Hudson MS, Deme D, Virion A. Purification of a novel flavoprotein involved in the thyroid NADPH oxidase Cloning of the porcine and human cdnas. J Biol Chem. 1999; 274:37265–37269. [PubMed: 10601291]
38. Geiszt M, Kopp JB, Varnai P, Leto TL. Identification of renox, an NAD(P)H oxidase in kidney. Proc Natl Acad Sci U S A. 2000; 97:8010–8014. [PubMed: 10869423]
39. Shiose A, Kuroda J, Tsuruya K, Hirai M, Hirakata H, Naito S, et al. A novel superoxide-producing NAD(P)H oxidase in kidney. J Biol Chem. 2001; 276:1417–1423. [PubMed: 11032835]
40. Suh YA, Arnold RS, Lassegue B, Shi J, Xu X, Sorescu D, et al. Cell transformation by the superoxide-generating oxidase Mox1. Nature. 1999; 401:79–82. [PubMed: 10485709]
41. Katsuyama M, Matsuno K, Yabe-Nishimura C. Physiological roles of NOX/NADPH oxidase, the superoxide-generating enzyme. J Clin Biochem Nutr. 2012; 50:9–22. [PubMed: 22247596]
42. Fukuyama M, Rokutan K, Sano T, Miyake H, Shimada M, Tashiro S. Overexpression of a novel superoxide-producing enzyme, NADPH oxidase 1, in adenoma and well differentiated adenocarcinoma of the human colon. Cancer Lett. 2005; 221:97–104. [PubMed: 15797632]
43. Laurent E, McCoy JW III, Macina RA, Liu W, Cheng G, Robine S, et al. Nox1 is over-expressed in human colon cancers and correlates with activating mutations in K-Ras. Int J Cancer. 2008; 123:100–107. [PubMed: 18398843]
44. Garrido-Urbani S, Jemelin S, Deffert C, Carnesecchi S, Basset O, Szyndralewiez C, et al. Targeting vascular NADPH oxidase 1 blocks tumor angiogenesis through a PPARalpha mediated mechanism. PLoS One. 2011; 6:14665.
45. Bonner MY, Arbiser JL. Targeting NADPH oxidases for the treatment of cancer and inflammation. Cell Mol Life Sci. 2012; 69:2435–2442. [PubMed: 22581366]
46. Kamata T. Roles of Nox1 and other Nox isoforms in cancer development. Cancer Sci. 2009; 100:1382–1388. [PubMed: 19493276]
47. Govindarajan B, Sligh JE, Vincent BJ, Li M, Canter JA, Nickoloff BJ, et al. Overexpression of Akt converts radial growth melanoma to vertical growth melanoma. J Clin Invest. 2007; 117:719–729. [PubMed: 17318262]

48. Shono T, Yokoyama N, Uesaka T, Kuroda J, Takeya R, Yamasaki T, et al. Enhanced expression of NADPH oxidase Nox4 in human gliomas and its roles in cell proliferation and survival. Int J Cancer. 2008; 123:787–792. [PubMed: 18508317]
49. Vaquero EC, Edderkaoui M, Pandol SJ, Gukovsky I, Gukovskaya AS. Reactive oxygen species produced by NAD(P)H oxidase inhibit apoptosis in pancreatic cancer cells. J Biol Chem. 2004; 279:34643–34654. [PubMed: 15155719]
50. Mochizuki T, Furuta S, Mitsushita J, Shang WH, Ito M, Yokoo Y, et al. Inhibition of NADPH oxidase 4 activates apoptosis via the AKT/apoptosis signal-regulating kinase 1 pathway in pancreatic cancer PANC-1 *c*ells. Oncogene. 2006; 25:3699–3707. [PubMed: 16532036]
51. Bhandarkar SS, Jaconi M, Fried LE, Bonner MY, Lefkove B, Govindarajan B, et al. Fulvene-5 potently inhibits NADPH oxidase 4 and blocks the growth of endothelial tumors in mice. J Clin Invest. 2009; 119:2359–2365. [PubMed: 19620773]
52. Block K, Gorin Y, Hoover P, Williams P, Chelmicki T, Clark RA, et al. NAD(P)H oxidases regulate HIF-2alpha protein expression. J Biol Chem. 2007; 282:8019–8026. [PubMed: 17200123]
53. Du J, Nelson ES, Simons AL, Olney KE, Moser JC, Schrock HE, et al. Regulation of pancreatic cancer growth by superoxide. Mol Carcinog. 2012
54. Arbiser JL, Petros J, Klafter R, Govindajaran B, McLaughlin ER, Brown LF, et al. Reactive oxygen generated by Nox1 triggers the angiogenic switch. Proc Natl Acad Sci U S A. 2002; 99:715–720. [PubMed: 11805326]
55. Yamaura M, Mitsushita J, Furuta S, Kiniwa Y, Ashida A, Goto Y, et al. NADPH oxidase 4 contributes to transformation phenotype of melanoma cells by regulating G2-M cell cycle progression. Cancer Res. 2009; 69:2647–2654. [PubMed: 19276355]
56. Lim SD, Sun C, Lambeth JD, Marshall F, Amin M, Chung L, et al. Increased Nox1 and hydrogen peroxide in prostate cancer. Prostate. 2005; 62:200–207. [PubMed: 15389790]
57. Szanto I, Rubbia-Brandt L, Kiss P, Steger K, Banfi B, Kovari E, et al. Expression of NOX1, a superoxide-generating NADPH oxidase, in colon cancer and inflammatory bowel disease. J Pathol. 2005; 207:164–176. [PubMed: 16086438]
58. Shinohara M, Shang WH, Kubodera M, Harada S, Mitsushita J, Kato M, et al. Nox1 redox signaling mediates oncogenic Ras-induced disruption of stress fibers and focal adhesions by down-regulating Rho. J Biol Chem. 2007; 282:17640–17648. [PubMed: 17435218]
59. Shinohara M, Adachi Y, Mitsushita J, Kuwabara M, Nagasawa A, Harada S, et al. Reactive oxygen generated by NADPH oxidase 1 (Nox1) contributes to cell invasion by regulating matrix metalloprotease-9 production and cell migration. J Biol Chem. 2010; 285:4481–4488. [PubMed: 20018867]
60. Fulton DJ. Nox5 and the regulation of cellular function. Antioxid Redox Signal. 2009; 11:2443–2452. [PubMed: 19331545]
61. Bedard K, Jaquet V, Krause KH. NOX5: from basic biology to signaling and disease. Free Radic Biol Med. 2012; 52:725–734. [PubMed: 22182486]
62. Kamiguti AS, Serrander L, Lin K, Harris RJ, Cawley JC, Allsup DJ, et al. Expression and activity of NOX5 in the circulating malignant B cells of hairy cell leukemia. J Immunol. 2005; 175:8424–8430. [PubMed: 16339585]
63. Brar SS, Corbin Z, Kennedy TP, Hemendinger R, Thornton L, Bommarius B, et al. NOX5 NAD(P)H oxidase regulates growth and apoptosis in DU 145 prostate cancer cells. Am J Physiol Cell Physiol. 2003; 285:C353–C369. [PubMed: 12686516]
64. Huang WC, Li X, Liu J, Lin J, Chung LW. Activation of androgen receptor, lipogenesis, and oxidative stress converged by SREBP-1 is responsible for regulating growth and progression of prostate cancer cells. Mol Cancer Res. 2012; 10:133–142. [PubMed: 22064655]
65. Zhou X, Li D, Resnick MB, Behar J, Wands J, Cao W. Signaling in H2O2-induced increase in cell proliferation in Barrett's esophageal adenocarcinoma cells. J Pharmacol Exp Ther. 2011; 339:218–227. [PubMed: 21750116]
66. Fu X, Beer DG, Behar J, Wands J, Lambeth D, Cao W. cAMP-response element-binding protein mediates acid-induced NADPH oxidase NOX5-S expression in Barrett esophageal adenocarcinoma cells. J Biol Chem. 2006; 281:20368–20382. [PubMed: 16707484]

67. Schramm A, Matusik P, Osmenda G, Guzik TJ. Targeting NADPH oxidases in vascular pharmacology. Vascul Pharmacol. 2012; 56:216–231. [PubMed: 22405985]
68. Jay DB, Papaharalambus CA, Seidel-Rogol B, Dikalova AE, Lassegue B, Griendling KK. Nox5 mediates PDGF-induced proliferation in human aortic smooth muscle cells. Free Radic Biol Med. 2008; 45:329–335. [PubMed: 18466778]
69. Ushio-Fukai M, Nakamura Y. Reactive oxygen species and angiogenesis: NADPH oxidase as target for cancer therapy. Cancer Lett. 2008; 266:37–52. [PubMed: 18406051]
70. Kawahara T, Lambeth JD. Phosphatidylinositol (4,5)-bisphosphate modulates Nox5 localization via an N-terminal polybasic region. Mol Biol Cell. 2008; 19:4020–4031. [PubMed: 18614798]
71. Kawahara T, Jackson HM, Smith SM, Simpson PD, Lambeth JD. Nox5 forms a functional oligomer mediated by self-association of its dehydrogenase domain. Biochemistry. 2011; 50:2013–2025. [PubMed: 21319793]
72. Guzik TJ, Chen W, Gongora MC, Guzik B, Lob HE, Mangalat D, et al. Calcium-dependent NOX5 nicotinamide adenine dinucleotide phosphate oxidase contributes to vascular oxidative stress in human coronary artery disease. J Am Coll Cardiol. 2008; 52:1803–1809. [PubMed: 19022160]
73. Sabeur K, Ball BA. Characterization of NADPH oxidase 5 in equine testis and spermatozoa. Reproduction. 2007; 134:263–270. [PubMed: 17660236]
74. El JA, Valente AJ, Lechleiter JD, Gamez MJ, Pearson DW, Nauseef WM, et al. Novel redox-dependent regulation of NOX5 by the tyrosine kinase c-Abl. Free Radic Biol Med. 2008; 44:868–881. [PubMed: 18160052]
75. Pandey D, Patel A, Patel V, Chen F, Qian J, Wang Y, et al. Expression and functional significance of NADPH oxidase 5 (Nox5) and its splice variants in human blood vessels. Am J Physiol Heart Circ Physiol. 2012; 302:H1919–H1928. [PubMed: 22427510]
76. BelAiba RS, Djordjevic T, Petry A, Diemer K, Bonello S, Banfi B, et al. NOX5 variants are functionally active in endothelial cells. Free Radic Biol Med. 2007; 42:446–459. [PubMed: 17275676]
77. Juhasz A, Antony S, Wu Y, Lu J, Jiang G, Liu H, et al. Effect of stable knockdown of NOX1 gene expression with siRNA in human colon cancer cells. Proceedings of the American Association for Cancer Research. 2012; Vol 53:742. Abstract no: 3066.
78. Wu Y, Antony S, Juhasz A, Lu J, Ge Y, Jiang G, et al. Up-regulation and sustained activation of Stat1 are essential for interferon-gamma (IFN-gamma)-induced dual oxidase 2 (Duox2) and dual oxidase A2 (DuoxA2) expression in human pancreatic cancer cell lines. J Biol Chem. 2011; 286:12245–12256. [PubMed: 21321110]
79. Wingler K, Hermans JJ, Schiffers P, Moens A, Paul M. Schmidt H.H. NOX1 2, 4, 5: counting out oxidative stress. Br J Pharmacol. 2011; 164:866–883. [PubMed: 21323893]

Highlights

- Characterization of the first mouse monoclonal Nox5 antibody.
- Detection of endogenous Nox5 protein in human UACC-257 melanoma cells.
- Substantial Nox5 overexpression in several human cancer tissues.
- Expression of Nox5 in non-malignant tissues is weak.

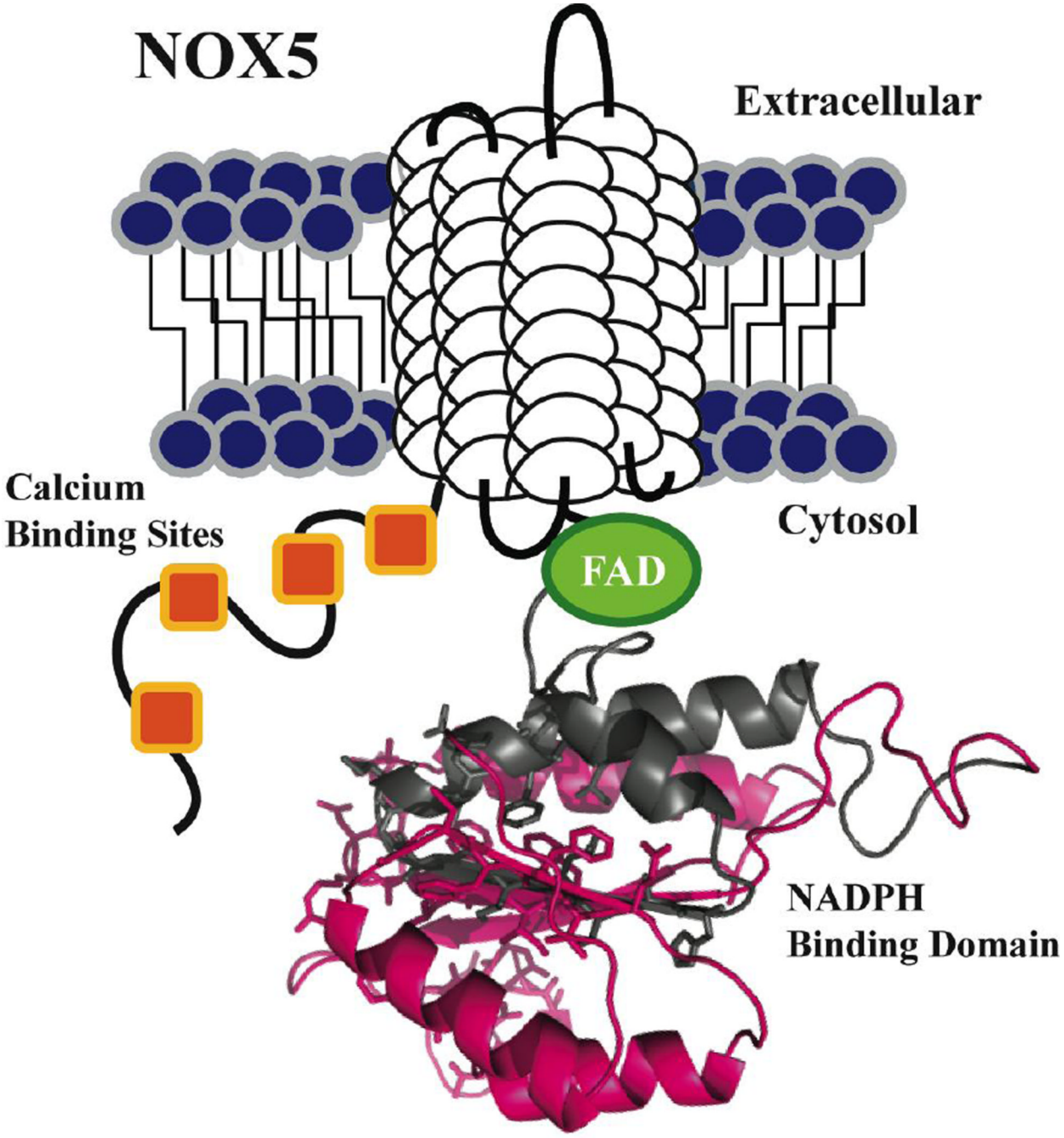

Fig. 1. Schematic view of the conserved structural features of the Nox5 protein

Each Nox5 isoform contains six putative trans-membrane (TM) domains (white cylindrical loops), with four N-terminal calcium binding sites (orange), and C-terminal FAD (green) and NADPH binding domains. The NADPH binding domain structural model was created by the SWISS-MODEL program server with hNox2 (PDB: 3A1F) as the template, visualized by Pymol software; the hNox2 and hNox5 NADPH binding domains share 36% amino acid sequence identity. The pink highlighted segment represents the antigen expressed for Nox5 antibody development (C-terminal 147 AA). Amino acids displayed as sticks represent the predicted NADPH binding site residues.

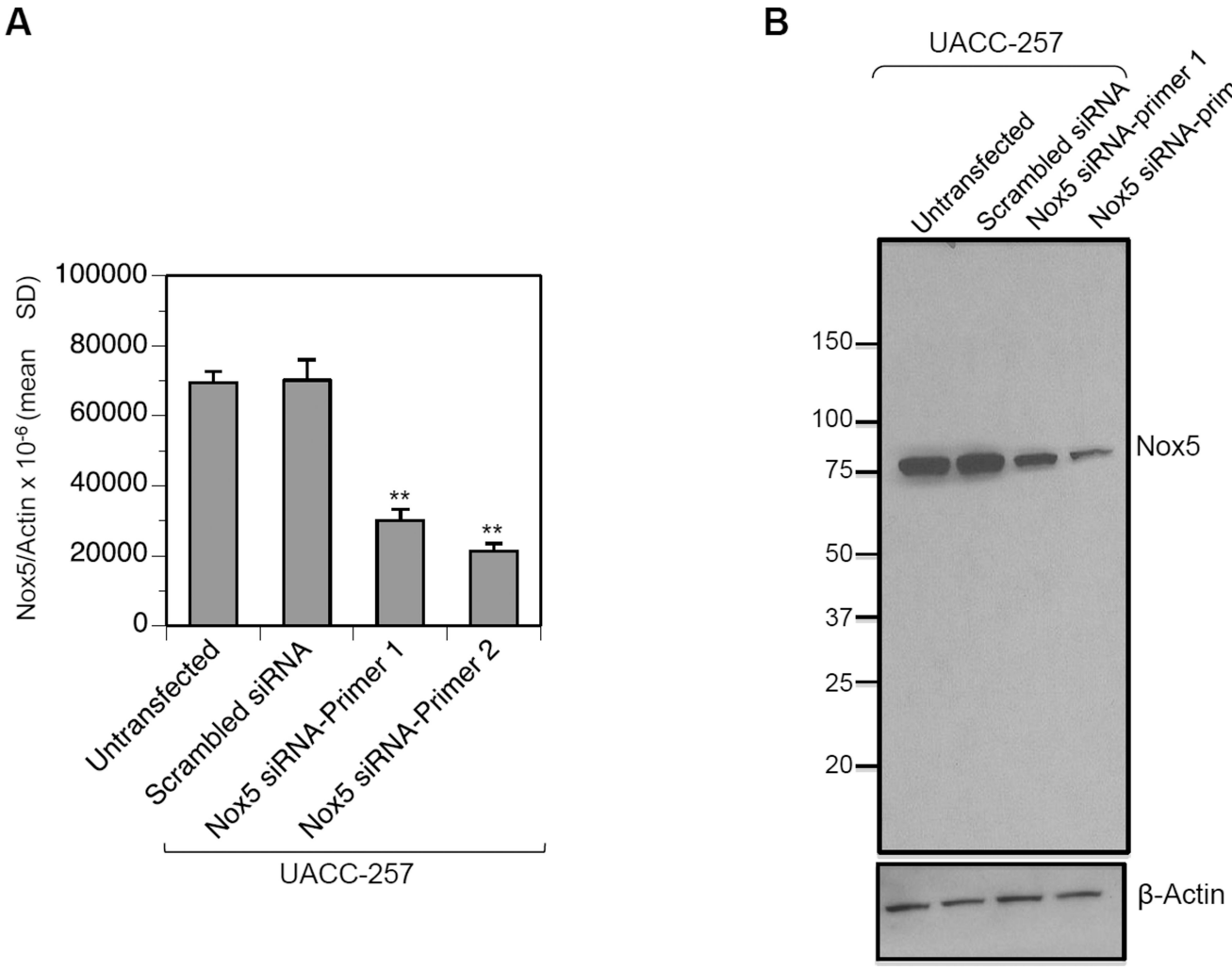

Fig. 2. Detection of Nox5 in UACC-257 human melanoma cells

Control scrambled siRNA and Nox5 specific siRNAs targeting different domains of human Nox5 were transiently transfected into the parental UACC-257 cells. Samples were processed 72 h after transfection to detect either Nox5 mRNA (**A**) by quantitative real time-PCR or Nox5 protein (**B**) by Western analysis. Nox5 mRNA levels are expressed relative to β-Actin. **, $p < 0.01$. Western analysis using the mouse monoclonal Nox5 antibody detects an ~ 75 kDa band corresponding to Nox5 protein.

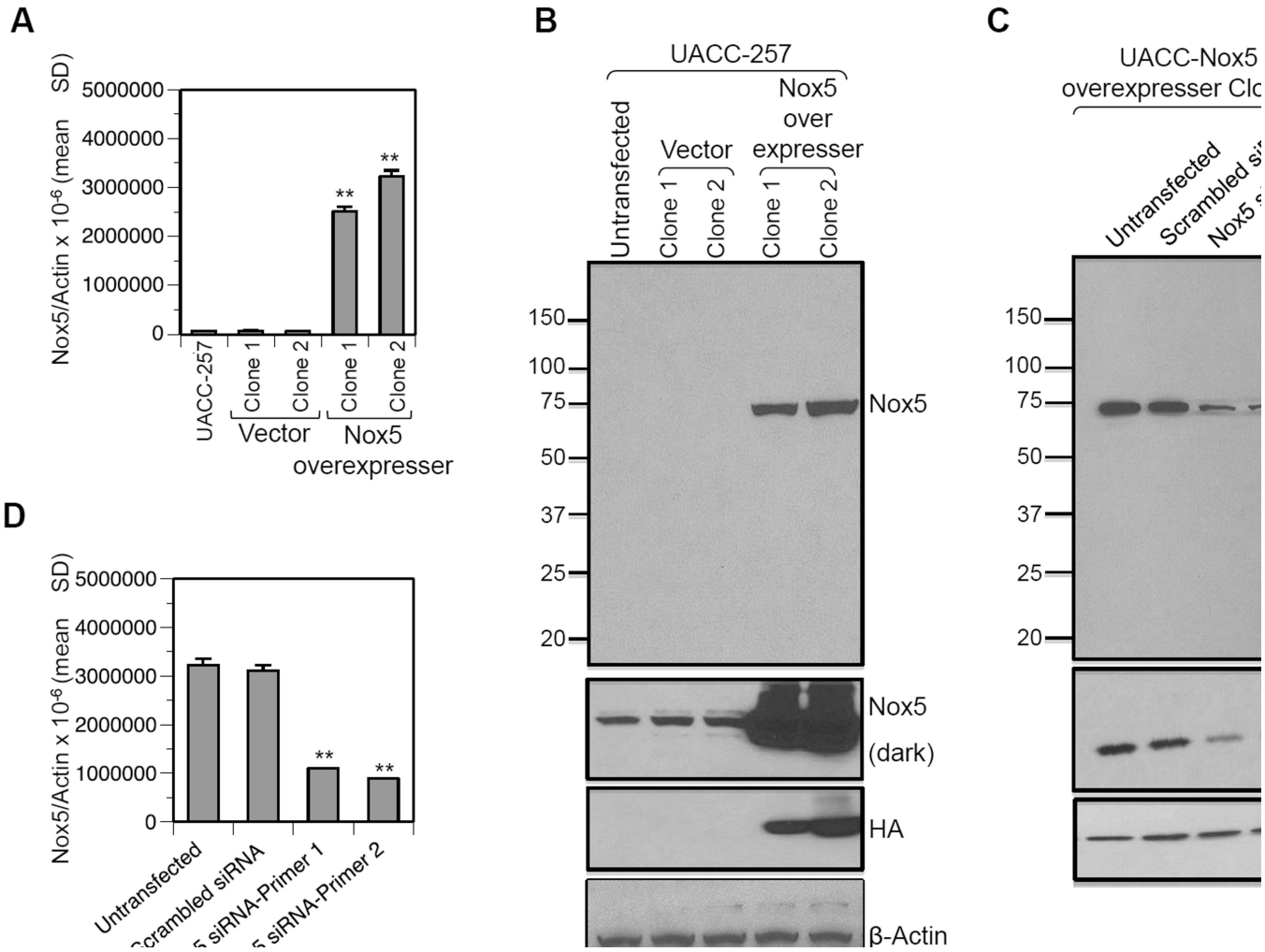

Fig. 3. Validation of the specificity of the Nox5 monoclonal antibody

UACC-257 cells were stably transfected with either the vector pcDNA 3.1 or pcDNA3-HA-Nox5β plasmid and selected with G418. Several clones were isolated, of which two vector clones (1 and 2) and two Nox5-overexpressing clones (1 and 2) were used for this study. Nox5 overexpression was confirmed both at the mRNA (**A**) and protein (**B**) levels. The HA tag expression confirmed the specificity of the Nox5 mouse monoclonal antibody for Nox5 overexpression. **C and D**, Transient knockdown of Nox5 expression in the stably Nox5 overexpressing clone 2 with either scrambled control or two different Nox5-specific siRNAs. The decrease in Nox5 expression was confirmed at the protein (**C**) and mRNA (**D**) levels. **, $p < 0.01$

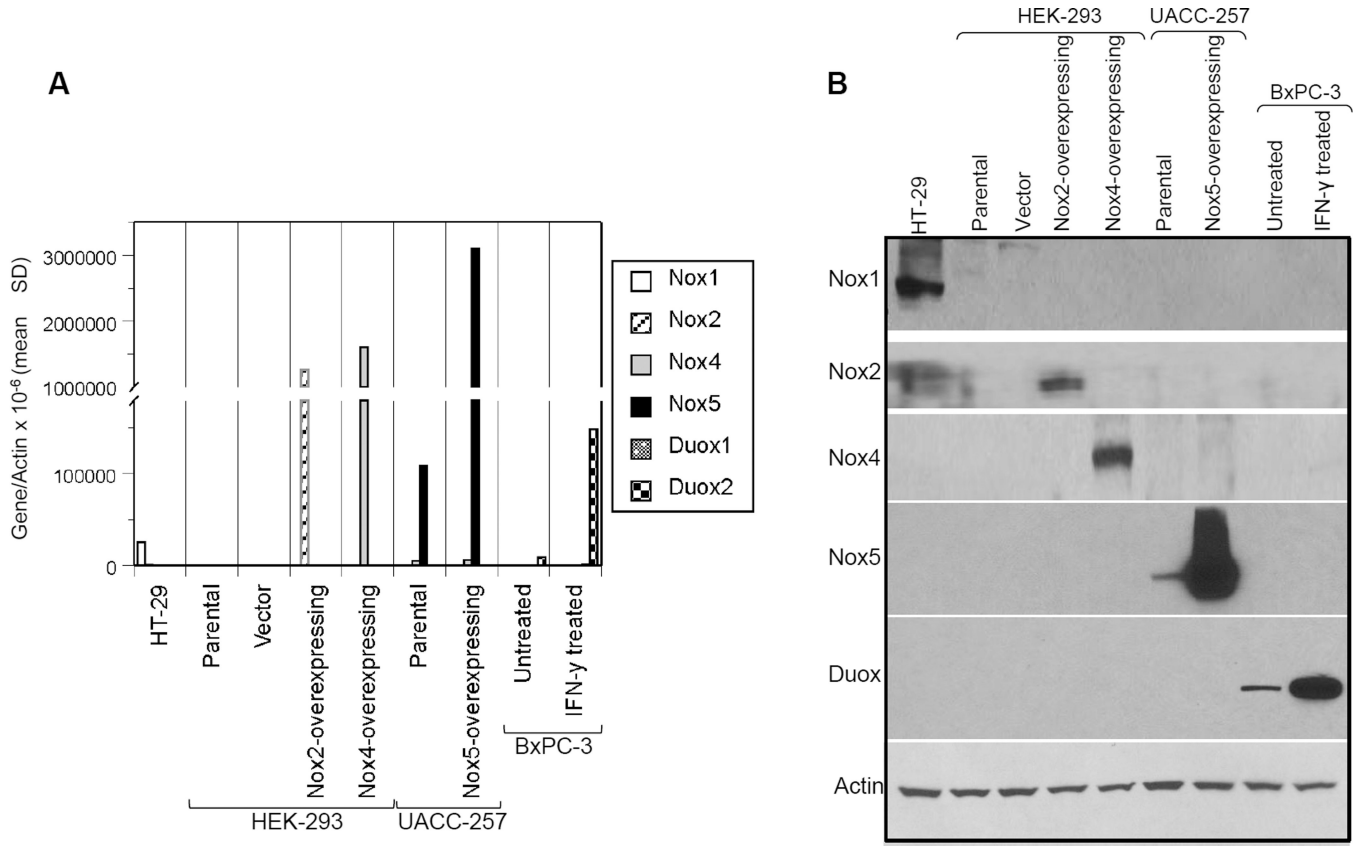

Fig. 4. Evaluation of cross-reactivity of the mouse monoclonal antibody to NADPH homologues of Nox5

RNA (**A**) and Western blot (**B**) analysis was carried out using samples positive for Nox1 (HT-29 colon cancer cell line), Nox2 (HEK-293 cells transiently transfected with DDK-tagged Nox2 plasmid), Nox4 (HEK-293 cells transiently transfected with Myc-tagged Nox4 plasmid), Nox5 (UACC-257 parental cells and Nox5 overexpressing cells), and Duox (BxPC-3 pancreatic cells treated with 25 ng/ml IFN-γ for 24 h) expression. Antibodies used to detect the various NADPH homologues are detailed in the Protocol section.

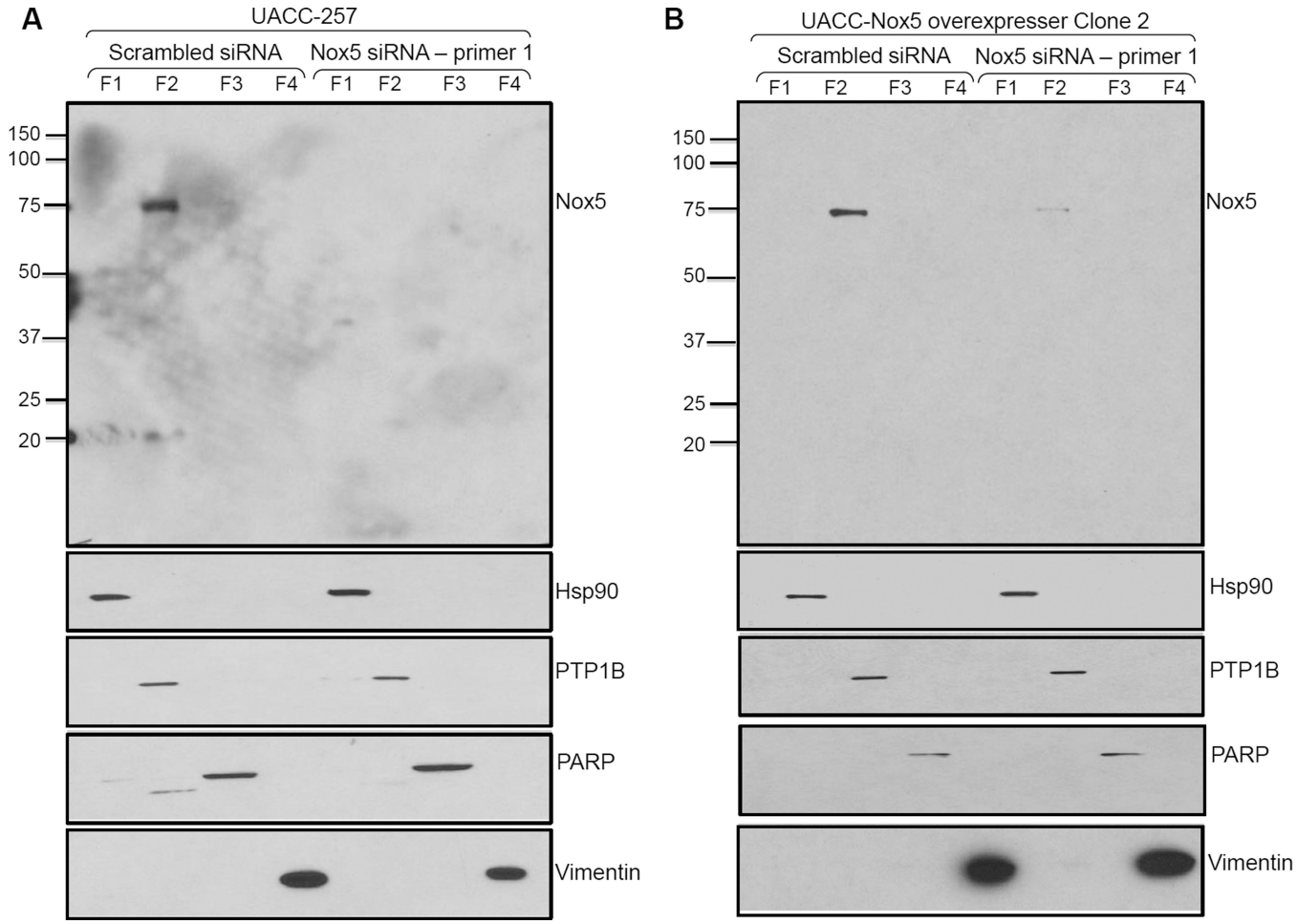

Fig. 5. Membrane localization of Nox5 protein in UACC-257 cells

Parental UACC-257 cells (**A**) or stably Nox5 overexpressing UACC-257 clone 2 (**B**) transiently transfected with either control scrambled or Nox5-specific siRNA were fractionated using the Qproteome cell compartment kit. Protein from fractions 1–4 (20 μg) was separated by SDS-PAGE. After Western blotting, proteins specific to each fraction were detected using Hsp90, PTP1B, PARP, and vimentin antibodies. Protein detection of Nox5 by the mouse monoclonal antibody was performed at 1:1000 and 1:10,000 dilutions for UACC-257 parental and Nox5 overexpressing cells, respectively. Nox5 was detected primarily in the membrane fraction of both parental and Nox5 over-expressing UACC-257 cells. F1: cytosolic proteins; F2: membrane proteins; F3: nuclear proteins; and F4: cytoskeletal proteins.

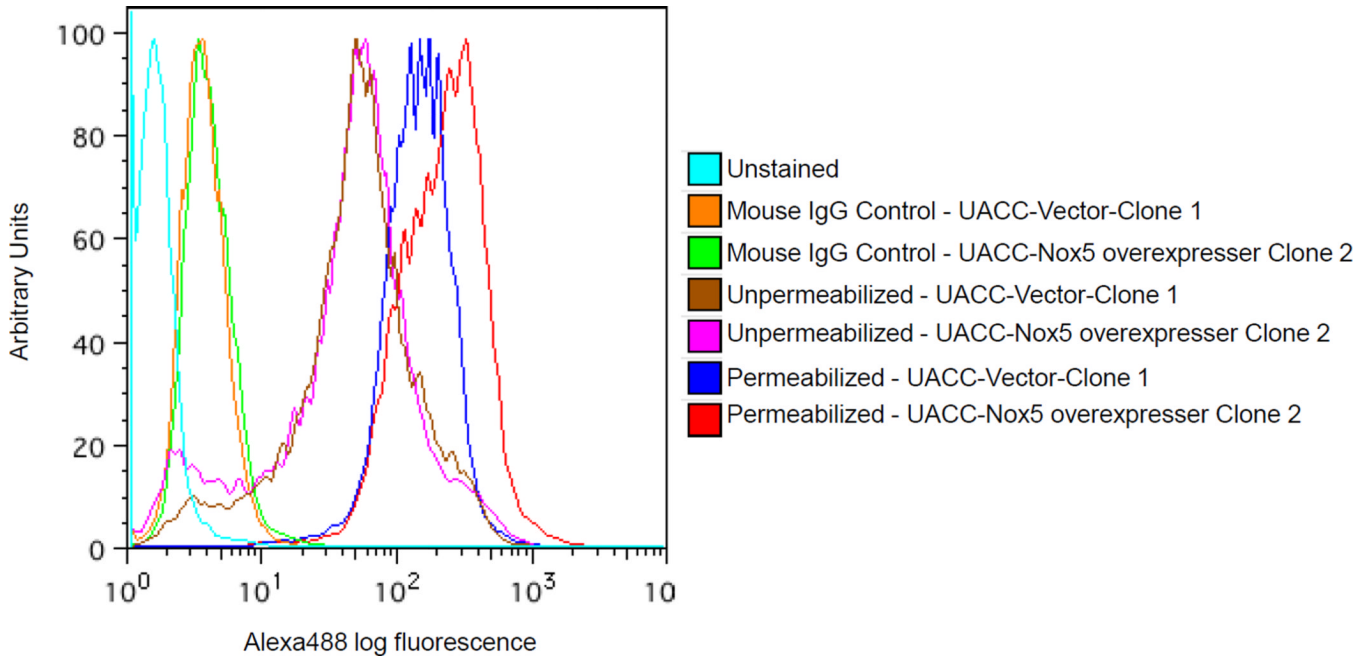

Fig. 6. Flow cytometric detection of Nox5 in UACC-257-Nox5 overexpressing cells

Log-phase UACC-257 cells that stably express Nox5 (Clone 2) or the vector control (Clone 1) were fixed, permeabilized, and labeled with 5 μg of purified Nox5 mouse monoclonal antibody as described in the Protocol section. Cells labeled with the antibody were staine d with Alexa Fluor 488 goat anti-mouse antibody (1:1000), and the fluorescence was detected by flow cytometry. Unstained cells and cells labeled with irrelevant mouse monoclonal IgG antibody (5 μg) represent background staining controls. Images are representative of at least 3 experiments.

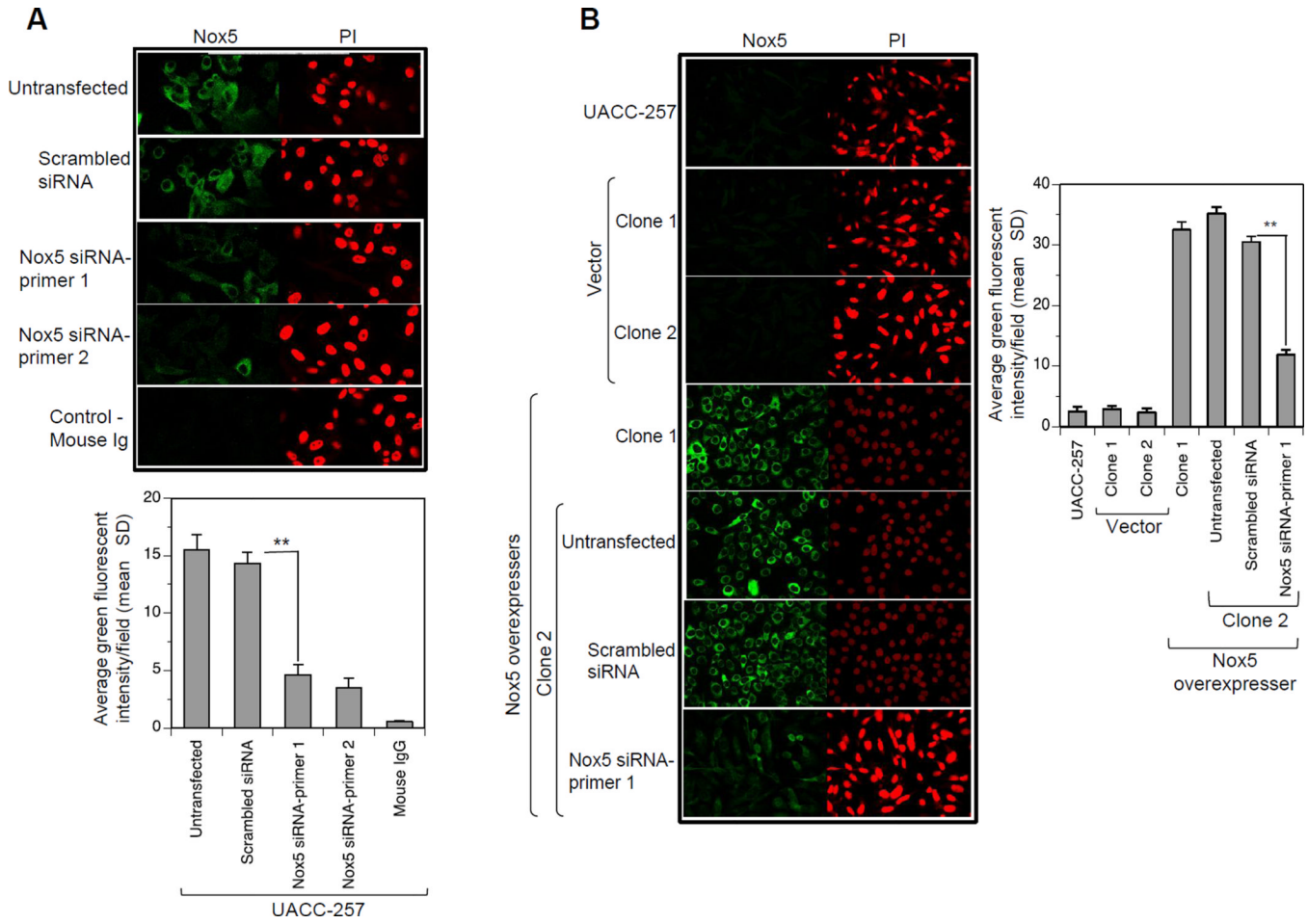

Fig. 7. Subcellular localization of Nox5 in UACC-257 cells by confocal microscopy

A, UACC-257 cells transfected with either scrambled control siRNA or Nox5-specific siRNAs 1 and 2 were plated on 4-well chamber slides. 72 h after transfection, the cells were fixed, permeabilized, and subjected to immunostaining as described in the Protocol section. Immunostaining was carried out with Nox5 mouse monoclonal antibody (1:1000) and Alexa Fluor 488 goat anti-mouse secondary antibody (*left panel; green*). Nuclear staining was observed with PI (*right panel; red*). For a negative control, cells were incubated with isotype-matched mouse IgG. Lower panel provides the quantitation of green fluorescent intensities/field for three separate experiments. **, $p < 0.01$ **B**, UACC-Nox5-overexpressing Clone 2 was transiently transfected with either scrambled control siRNA or Nox5-specific siRNA and processed as above along with the parental UACC-257, the vector clones (1 and 2) and the Nox5-overexpresser clone 1, with the exception that the mouse monoclonal antibody was used at a 1:10,000 dilution. Representative confocal images of Nox5 mAb binding as detected by FITC fluorescence (*green*) and the corresponding nuclear fields (red) are shown. Right panel provides the quantitation of green fluorescent intensities/field for three separate experiments. **,$p < 0.01$

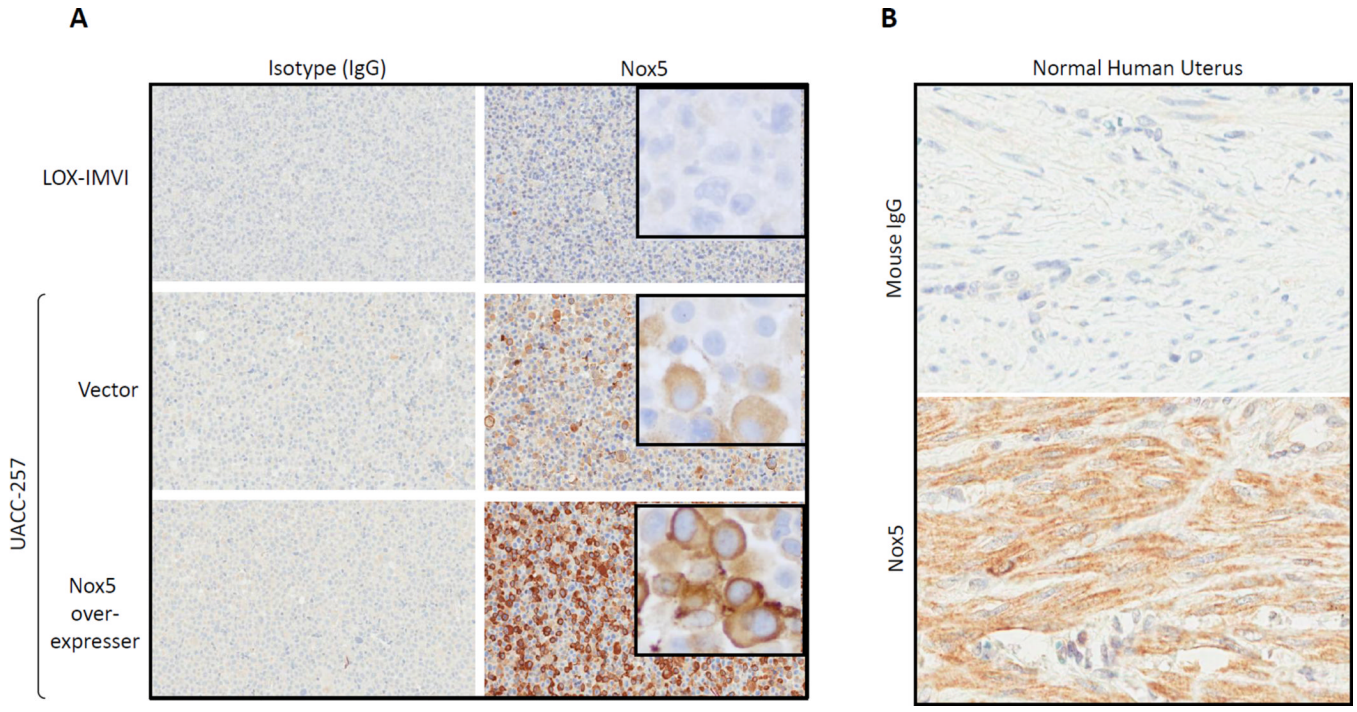

Fig. 8. Immunohistochemical localization of Nox5

A) Immunohistochemical staining profile with Isotype control (IgG) on the left and Nox5 mouse monoclonal antibody on the right. LOX-IMVI melanoma cell line is negative for Nox5 staining. UACC-257 vector control cells have patchy reactivity of moderate intensity (20X) for Nox5. ***Insert*** - cytoplasmic staining concentrated toward the membrane (40X). Nox5 over-expresser (Clone 2) has diffuse and strong immunoreactivity for Nox5 expression (20X). ***Insert*** -cytoplasmic staining concentrated toward the membrane (40X). **B**) Immunohistochemistry performed on normal human uterus demonstrated diffusely positive staining for Nox5 in uterine smooth muscle (bottom panel); staining with the isotype control was negative (top panel).

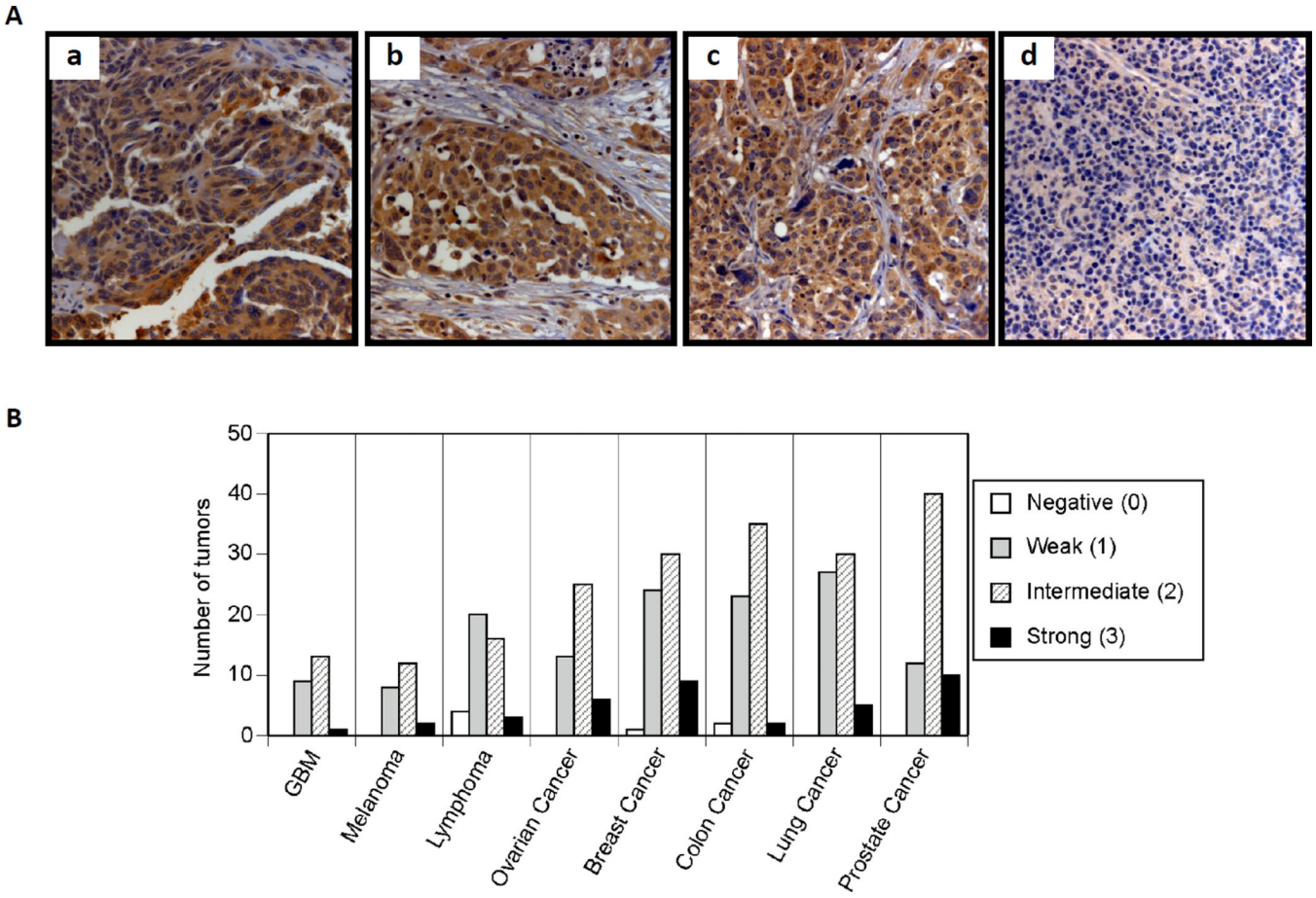

Fig. 9. Immunohistochemistry for Nox5 performed on a multi-tumor tissue microarray

A) Immunohistochemistry for Nox5, demonstrating expression in a) ovarian papillary serous adenocarcinoma, b) adenocarcinoma of the prostate, c) adenocarcinoma of the lung carcinoma and, d) lack of expression in lymphoma. All images are 250X magnification. **B**) Graphical representation of the distribution of the 382 evaluable tumor samples for cytoplasmic staining of Nox5 into 0, 1, 2, and 3, corresponding to negative, weak, intermediate, and strong staining respectively. GBM, Glioblastoma Multiforme

Table 1

Distribution of expression levels of Nox5 in human malignancies.

Tumor Type (MTA–3)	Negative (0–1)	Positive (2–3)
Glioblastoma Multiforme (GBM)	9 (39%)	14 (61%)
Melanoma	8 (36%)	14 (64%)
Lymphoma	24 (56%)	19 (44%)
Ovarian Cancer	13 (30%)	31 (70%)
Breast Cancer	25 (39%)	39 (61%)
Colon Cancer	25 (40%)	37 (60%)
Lung Cancer	27 (44%)	35 (56%)
Prostate Cancer	12 (19%)	50 (81%)

Tumors that were negative (0) or weak (1) for Nox5 staining were considered Negative and those that stained intermediate 2) to strong (3) as Positive. Represented within brackets are the relative percentages of tumors,